Received: 13 December 2019 | Revised: 3 April 2020 | Accepted: 8 April 2020

DOI: 10.1111/bcpt.13417

ORIGINAL ARTICLE

BCPT Basic & Clinical Pharmacology & Toxicology

# Riluzole: Anti-invasive effects on rat prostate cancer cells under normoxic and hypoxic conditions

**Nahit Rizaner[1,2] | Sercan Uzun[3] | Scott P. Fraser[1] | Mustafa B. A. Djamgoz[1,2] | Seyhan Altun[3,4]**

[1]Department of Life Sciences, Neuroscience Solutions to Cancer Research Group, Imperial College London, London, UK

[2]Biotechnology Research Centre, Cyprus International University, Haspolat, Turkey

[3]Department of Biology, Faculty of Science, Istanbul University, Istanbul, Turkey

[4]Department of Molecular Biology and Genetics, Faculty of Science and Letters, Istanbul Kultur University, Istanbul, Turkey

**Correspondence**
Mustafa B. A. Djamgoz, Department of Life Sciences, Neuroscience Solutions to Cancer Research Group, Sir Alexander Fleming Building, Imperial College London, South Kensington Campus, London SW7 2AZ, UK.
Email: m.djamgoz@imperial.ac.uk

**Funding information**
Istanbul University Research Fund Istanbul University Research Fund , Grant/Award Number: 21348; Pro Cancer Research Fund

**Abstract**

Anti-invasive effects of riluzole and ranolazine, a neuro-protectant and an anti-anginal drug, respectively, on Mat-LyLu rat prostate cancer (PCa) cells were tested in vitro (a) at non-toxic doses and (b) under both normoxic and hypoxic conditions, the latter common to growing tumours. Tetrodotoxin (TTX) was used as a positive control. Hypoxia had no effect on cell viability but reduced growth at 48 hours. Riluzole (5 μmol/L) or ranolazine (20 μmol/L) had no effect on cell viability or growth under normoxia or hypoxia over 24 hours. Matrigel invasion was not affected by hypoxia but inhibited by TTX, ranolazine and riluzole under a range of conditions. The expression of Nav1.7 mRNA, the prevailing, pro-invasive voltage-gated sodium channel α-subunit (VGSCα), was up-regulated by hypoxia. Riluzole had no effect on Nav1.7 mRNA expression in normoxia but significantly reduced it in hypoxia. VGSCα protein expression in plasma membrane was reduced in hypoxia; riluzole increased it but only under hypoxia. It was concluded (a) that riluzole and ranolazine have anti-invasive effects on rat PCa cells and (b) that Nav1.7 mRNA and protein expression can be modulated by riluzole under hypoxia. Overall, therefore, riluzole and ranolazine may ultimately be "repurposed" as anti-metastatic drugs against PCa.

**KEYWORDS**

hypoxia, invasion, prostate cancer, riluzole, voltage-gated sodium channel

## 1 | INTRODUCTION

Functional up-regulation of voltage-gated sodium channel (VGSC) expression in cancer cells of strong metastatic potential was discovered in rat prostate cancer (PCa) and then confirmed for human cells and tissues.[1-4] In both rat and human PCa, the predominant VGSC subtype was shown to be Nav1.7.[1,3-6] The VGSC activity was found to promote a range of metastatic cell behaviours, including lateral motility, transverse migration, galvanotaxis, endocytic membrane activity and Matrigel invasion.[2-4,7-14] Indeed, from an "overexpression" study on a non-metastatic cell line, it was proposed that the VGSC expression was "necessary and sufficient" for cellular invasiveness in human PCa cells.[7] Furthermore, it was reported for the rat strongly metastatic PCa cell line Mat-LyLu that VGSC activity can auto-regulate channel protein trafficking and functional expression, thus also promoting the progression of PCa via a positive feedback mechanism.[8] In vivo, local injection of the highly specific VGSC blocker, tetrodotoxin (TTX), into

These authors Rizaner and Uzun have contributed to this study equally and are listed alphabetically.

primary tumours significantly reduced metastases to lungs and prolonged survival.[14] In contrast, proliferative activity in vitro and in vivo was not affected by VGSC blockage consistent with the notion that primary tumorigenesis (ie proliferation) and metastasis (ie invasion) are controlled differently, even partially independently.[15-18] Finally, quantitative analysis of "receiver operator characteristics" (ROC) in human biopsy tissues suggested that Nav1.7 mRNA expression had sufficient selectivity and specificity to serve as an effective biomarker of PCa.[6]

Consequently, VGSC blocking drugs have been proposed as potential anti-cancer/metastatic agents.[19-21] These include local anaesthetics, anti-convulsants and anti-arrhythmics.[22-24] Most work has been done on breast cancer (BCa). Thus, Yang et al showed that the anti-epileptic drug phenytoin suppressed BCa invasiveness in vitro and metastasis in vivo.[25] Another interesting agent is the anti-excitatory and neuroprotective drug, riluzole (2-amino-6-trifluoromethoxy benzothiazole) [eg[26]]. Its use, under the brand name "Rilutek," was approved for the treatment of amyotrophic lateral sclerosis (ALS) in USA and Europe [eg[27]]. Interestingly, ALS and cancer have been shown to share some genetic characteristics.[28] Riluzole inhibited proliferation and migration, and induced apoptosis in cells of rhabdomyosarcoma/medulloblastoma, neuroblastoma, astrocytoma, glioma, colon cancer, lung cancer, thyroid carcinoma, leukaemia, erythroleukaemia and multiple myeloma.[29] Riluzole has also been found to inhibit proliferation and invasion of BCa and melanoma cells.[30,31] Finally, ranolazine (brand name "Ranexa") is used clinically against angina.[32] This drug has also been shown to suppress invasiveness in vitro (BCa) and metastasis in vivo (BCa and PCa).[16,33]

The main aim of the present study was to determine the possible anti-invasive effects of riluzole on the strongly metastatic rat PCa model, Mat-LyLu cell line. In some experiments, ranolazine and the isogenic weakly metastatic AT-2 cells devoid of functional VGSC expression were also used for comparison. The specific aims were as follows: (a) to determine the effects of riluzole on cellular viability, proliferation and invasiveness; and (b) to test whether riluzole would regulate VGSC mRNA and protein levels. Experiments were carried out under normoxic and hypoxic conditions, the latter known generally to occur in growing tumours and to promote metastasis [eg[34,35]]. Importantly, we aimed to study the cells' behaviour under "non-killing" conditions which can ultimately make cancer cells more aggressive [eg[36,37]].

## 2 | MATERIALS AND METHODS

This study involved several procedures as follows. Unless stated otherwise, all chemicals were obtained from Sigma-Aldrich.

### 2.1 | Cell culture

Mat-LyLu and AT-2 cells were grown to near confluence and serially passaged every 7-14 days (up to 15-20 passages), as described earlier.[2,15] All cells were seeded into 100-mm Falcon tissue culture dishes and grown in an incubator at 37°C, 100% relative humidity and 5% $CO_2$. Hypoxia (2% $O_2$) was induced for 24-48 hours in a dedicated incubator (Micro Galaxy, RS Biotech Laboratory Equipment Ltd).

### 2.2 | Pharmacology

Cells were treated pharmacologically under normoxic or hypoxic conditions. Riluzole was prepared as a stock solution (60 mmol/L) in 30% DMSO (v/v in $H_2O$) and stored at −20°C. The stock solution was diluted to a range of concentrations (1-10 μmol/L) in culture medium shortly before application. Riluzole was shown to be safe for human beings at concentrations up to 10 μmol/L.[38,39] The corresponding concentrations of DMSO were used as matching controls. The maximal final concentration of DMSO was 0.005%. Ranolazine was made as a stock solution of 2 mmol/L in normal culture medium and diluted to 20 μmol/L as the working concentration. Tetrodotoxin (TTX) was obtained from Alomone Labs, dissolved in normal medium as aliquots of 3132 μmol/L and diluted to the working concentration as required. Culture medium ± pharmacological agent(s) were replaced every 24 hours if experiments lasted longer.

### 2.3 | Functional assays

#### 2.3.1 | Cell viability

Trypan blue exclusion assay was used as described previously.[10] Briefly, cells were plated into 35-mm Falcon tissue culture dishes at a density of $3 \times 10^4$/mL and allowed to settle overnight. After drug treatment, cell culture medium ± pharmacological agent was then replaced with 0.1% trypan blue in normal culture medium. After incubation for 10 minutes at 37°C, the solution was replaced with 1 mL fresh cell culture medium and the cells were viewed at 400× magnification under an inverted microscope (Carl Zeiss). For each treatment, the percentage of dead cells was determined from 30 randomly selected fields of view which had at least 30 cells. This procedure was repeated on three separate dishes. Data are presented as averages of 3 × 30 measurements.

#### 2.3.2 | Growth

Any change in cell number after long-term pharmacological treatment was assessed by the colorimetric

3-[4,5-dimethylthiazol-2-yl]-2,5-diphenyltetrazolium bromide (MTT) (Alfa Aesar) method as described previously.[2] Briefly, cells ($4 \times 10^4$) were plated in 12-well Falcon tissue culture plates (Becton Dickinson) allowed to settle for 24 hours and treatment was applied. The culture medium was then replaced with control medium containing 1 mg/mL MTT and incubated at 37°C. After 2 hours, the medium was replaced with 0.89 mL DMSO and 0.11 mL glycine buffer (0.1 mol/L glycine and 0.1 mol/L NaCl, pH 10.5) for 10 minutes. The absorbance of the staining was measured in the dark at 570 nm on a multi-well plate reader (ELx800, BioTek Instruments/Thermo Fischer Scientific Multiskan). Measurements were made in duplicates, and each treatment was repeated at least three times. Absorbances were normalized to the corresponding control-DMSO group. The zero-hour recording was taken to be the first measurement made after the initial 24 hours. Standard calibration curves were created to verify the linearity of the relationship between cell number and absorbance, serial dilutions starting from $1.2 \times 10^6$ cells. Growth ("cell number") was assumed to represent proliferation if there was no change in cell viability.

### 2.3.3 | Matrigel invasion

Transwell migration filters (with 8-μm pores), pre-coated with 1.25 mg/mL Matrigel (Becton Dickinson), were incubated at 37°C for 30 minutes before plating 1-4 $\times 10^5$ cells, as described previously [eg[2,3]]. Cells were incubated in medium ± pharmacological agent in 0.5%-5% FBS chemotactic gradient for 24 hours. Afterwards, non-invaded cells were removed from the top by swabbing the upper surface of the Transwell filter. Invaded cells were fixed with 100% ice-cold methanol for 15 minutes and then stained with 0.5% (w/v) crystal violet in 25% methanol for 15 minutes at room temperature. Filters were washed in water and air-dried for 1 hour. For each insert, three randomly selected fields of view were photographed using a digital camera (Power-shot G5, Canon) mounted on an inverted microscope (Axiovert 200, Zeiss) at 100× magnification. Images were analysed using ImageJ software (NIH). Experiments were performed in duplicates. The average cell count from the six fields of view represented one measurement. Experiments were repeated independently at least three times, and results were normalized relative to the control.

## 2.4 | Molecular biology

Extraction of RNA and synthesis of cDNA were performed as described previously.[40] For real-time PCR, 10 μL of QuantiTech SYBR Green PCR mix (Qiagen), 5 μL cDNA, 0.5 μmol/L of both sense and antisense primers (Eurofins Genomics UK) were mixed. The final volume was made up to 20 μL with RNase- and DNase-free distilled water. The primer sequences were as follows (designed here unless indicated):

rNav1.7: 5′-TGACTTGGAAGCTGGGAAAC-3′ (F);
5′-TTCCAAGGGTCACGGAGGA-3′ (R)
β-actin: 5′-TCCCTGGAGAAGAGCTACGA-3′ (F);
5′-ATCTGCTGGAAGGTGGACAG-3′ (R)[41]
Cytb5R: 5′-ACACGCATCCCAAGTTTCCA-3′ (F);
5′-CATCTCCTCATTCACGAAGC-3′ (R)[42]

Amplification was performed on a DNA Engine Opticon 2 System (MJ Research). Reaction was started by heating at 95°C for 15 minutes to activate HotStar Taq. This was followed by 3-step 40 cycles of 95°C for 30 seconds, 60°C (annealing temperature) for 30 seconds and 72°C for 30 seconds. In order to verify the product composition, a melting curve was carried out from 65 to 95°C in 0.3°C steps at the end of the reaction. For each cDNA sample, duplicate reactions were performed for both the target gene and the normalizing (control) gene (Cytb5R or β-actin) simultaneously. Each set of reactions also included a non-template control, where the cDNA was replaced by DNase- and RNase-free distilled water. Standard calibration curves for each target gene using four serial dilutions of a cDNA template were also performed. Opticon Monitor 2 software (MJ Research) was used to determine the threshold amplification cycles (CT's). PCR product sizes were controlled visually by agarose gel electrophoresis.

## 2.5 | Immunocytochemistry, confocal microscopy and image analysis

These procedures were as described in detail previously.[8] Essentially, cells were plated onto poly-L-lysine-coated glass coverslips ($5 \times 10^4$ cells per coverslip), treated pharmacologically overnight and fixed in 4% paraformaldehyde (PFA)/PBS for 15 minutes. Where appropriate, cells were then labelled with 20 μg/100 μL fluorescein isothiocyanate (FITC)-conjugated concanavalin A (in 5% w/v BSA/PBS) as a plasma membrane marker. After washing, permeabilization in 0.1% (w/v) saponin/PBS and "blocking" with 5% BSA/PBS, cells were incubated for 1 hour with primary antibody (pan-VGSC, rabbit polyclonal, 1:100 dilution in 5% (w/v) in BSA/PBS; Upstate). Secondary antibody (in 5% w/v BSA/PBS) was goat anti-rabbit conjugated with Alexa-568. After washing, coverslips were mounted in VECTASHIELD medium (Vector Laboratories) and stored at 4°C in dark for 16 hours before microscopy. The following negative controls were used to test for the specificity of the primary antibody: (a) 5% BSA/PBS; (b) non-specific rabbit IgG (0.002-0.004 μg/μL non-specific rabbit IgG; Agilent Dako); and (c) pre-absorbed primary antibody (primary antibody

pre-absorbed with 5× excess of the immunizing peptide for 30 minutes at room temperature).

Immunostained cells were examined under a Leica SP5 MP/ Leica TCS-NT Ar/He laser scanning microscope with ×63 oil immersion objective (Leica Microsystems). Images (1024 × 1024 pixels) were obtained simultaneously from the two channels using a confocal pinhole of 229.96 μm and analysed using the Leica LAS AF Lite software. The expression of VGSCα protein in plasma membrane was assessed using the "freeform" function.[8] Signal intensity, in arbitrary unit (AU), was measured in the region of interest marked by the limits of the concanavalin A staining. Measurements were taken from a minimum of 30 randomly chosen cells in total per condition, from at least three independent experiments.

## 2.6 | Data analyses

Data were presented as means ± standard errors of the mean (SEMs) or as median values with 5 and 95% percentiles, interquartile ranges and outliers. Data analyses were performed using Excel 2003 (Microsoft Corporation), Origin 9 (OriginLab Corporation), SPSS version 21 (SPSS) and SigmaStat 2.0 (Systat Software Inc). Pairwise statistical significance was determined using unpaired Student's *t* test, or Mann-Whitney rank-sum test, as appropriate.[43] For comparisons involving more than two groups, statistical significance was determined using analysis of variance (ANOVA) followed by Tukey's post hoc analysis or Kruskal-Wallis analysis of variance as appropriate.[43] Real-time PCR data were analysed using the $2^{-\Delta\Delta C_T}$ method.[44] Results were considered significant at $P < .05$ (*) and highly significant at $P < .01$ (**). Specific details are given in figure legends.

# 3 | RESULTS

Effects of riluzole on several different characteristics of the strongly metastatic Mat-LyLu cells were studied under normoxic and hypoxic conditions. Some initial comparisons were made with ranolazine and the weakly metastatic syngeneic AT-2 cells.

## 3.1 | Cellular viability and growth

Firstly, we determined the possible effects of hypoxia alone on Mat-LyLu and AT-2 cells. Hypoxia (2% $O_2$) applied for up to 48 hours had no discernible effect on the morphology or viability of either cell line. Treatment with TTX (1 μmol/L) in normoxia or hypoxia also did not affect viability of either cell line (not shown). As regards "growth," there was no effect of hypoxia alone on Mat-LyLu cells at 24 hours, but a significant (30%) decrease was observed at 48 hours ($P < .05$; n = 4; Figure 1A). This effect became bigger (59%) at 72 hours (not shown). In contrast, hypoxia had no effect on the "growth" of AT-2 cells, even at 72 hours ($P > .05$; n = 3; Figure 1B). Also, TTX had no effect on the "growth" of either cell line under normoxic and hypoxic conditions ($P > .05$; n ≥ 3; Figure 1A,B).

These results largely confirmed earlier studies showing lack of effect of TTX on viability and proliferative activity of Mat-LyLu and AT-2 cells and extended the findings to hypoxia. The remaining experiments were performed on Mat-LyLu cells.

Treatment with riluzole (up to 10 μmol/L) for 24 hours was not toxic to Mat-LyLu cells under normoxic or hypoxic conditions (Figure 1C). Similarly, 20 μmol/L ranolazine was not toxic (not shown). When the treatment period was extended to 48 hours, 10 μmol/L riluzole still had no effect on Mat-LyLu cell viability under normoxia (Figure 1C). Any effect of riluzole or ranolazine on Mat-LyLu cell viability over 48 hours in hypoxia was not tested since hypoxia alone over this period had an inhibitory effect on cell number (Figure 1A).

No significant change was recorded in "growth" of Mat-LyLu cells after 24 hours of treatments with riluzole (up to 5 μmol/L) in normoxic and hypoxic conditions (n ≥ 3 each; Figure 1D). Similarly, ranolazine had no effect (not shown). Since the cells remained viable under these conditions, it was concluded that Mat-LyLu cells' proliferative activity was not affected by riluzole (at 5 μmol/L) or ranolazine applied for 24 hours under normoxic or hypoxic conditions. Increasing the riluzole concentration to 10 μmol/L significantly decreased the Mat-LyLu cell number under normoxia time dependently by 30% (24 hours) and 52% (48 hours; $P < .05$ cf. respective control, for both; n ≥ 4; Figure 1D). Under hypoxia (24 hours), however, 10 μmol/L riluzole did not affect cell number, hence proliferation (Figure 1D).

In conclusion, in order to avoid any complication of the treatments used on cell viability or growth, the subsequent experiments on invasiveness were designed as follows: (a) all hypoxic treatments were restricted to 24 hours. (b) Riluzole treatments were restricted to 1-5 μmol/L (up to 48 hours in normoxia; 24 hours in hypoxia). (c) Ranolazine (20 μmol/L) was used for comparison under 24 hours in normoxia or hypoxia.

## 3.2 | Matrigel invasion

Boyden chamber (Matrigel) assays were performed to determine the possible anti-invasiveness effects of the pharmacological agents on Mat-LyLu cells. Treatment with 1 μmol/L

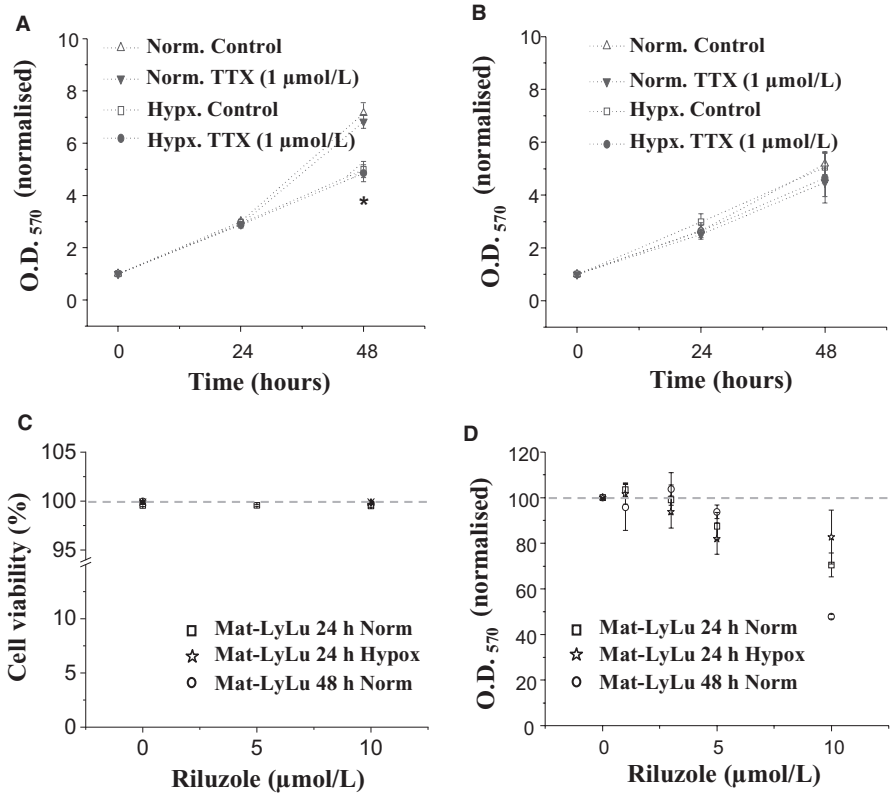


**FIGURE 1** Cell viability and growth. Effects of normoxia and hypoxia and 1 µmol/L TTX on A, Mat-LyLu and B, AT-2 cell growth over 24 and 48 h. C, Lack of effects of riluzole (<10 µmol/L) on viability of Mat-LyLu cells over 48 h. D, Effects of 1-10 µmol/L riluzole on cell growth. For parts (C) and (D), treatments lasted 24 or 48 h (normoxia), and 24 h (hypoxia). Data are presented as means ± SEMs (n ≥ 3). Statistical significance (A): $P < .05$ (*) for control vs. treatment at 48 h

TTX for 24 hours (used as a positive control) significantly reduced invasiveness by 50% and 53% under normoxic and hypoxic conditions, respectively ($P < .01$ and $P < .05$ cf. non-treated controls, respectively; n = 7-10; Figure 2A,B). Similarly, ranolazine significantly reduced invasiveness by 55% and 66% in normoxia and hypoxia, respectively ($P < .01$ and $P < .05$ cf. non-treated controls, respectively; n = 4-8; Figure 2A,B). Hypoxia by itself had no effect on invasiveness, apparent in the controls of both the TTX and the ranolazine treatments ($P = .78$ and $P = .59$, respectively; n = 7-12; Figure 2B). Riluzole (1-5 µmol/L) had no effect on invasion over 24 h under either condition ($P > .05$ cf. DMSO control, for all comparisons; n = 3 each; Figure 2A,B). Increasing the treatment period to 48 hours under normoxia resulted in a dose-dependent inhibitory effect by 7%-45%. This reached significance at 5 µmol/L riluzole ($P < .05$; n = 4 each; Figure 2A). The inhibitory effect of TTX was maintained at 48 hours (not shown). Any effect of riluzole, TTX or ranolazine under hypoxia over 48 hours could not be tested due to the inhibitory effect of hypoxia alone on cell growth, observed earlier (Figure 1A).

### 3.3 | Nav1.7 mRNA level and VGSCα protein expression

We then questioned whether VGSC (Nav1.7) mRNA and protein levels would change under the pharmacological treatments. For this, we tested riluzole as an example. In these experiments, Mat-LyLu cells were treated with 1-5 µmol/L riluzole for 24 hours under normoxic or hypoxic conditions. Nav1.7 mRNA expression was quantified relative to two different control genes (Cytb5R and β-actin) which gave similar results (Figure 3A). Hypoxia by itself increased Nav1.7 mRNA expression by >400% ($P < .001$; n = 3; Figure 3B). Riluzole, even at the highest concentration (5 µmol/L) tested, had no effect on Nav1.7 mRNA expression under normoxia (Figure 3B, light bars). Under hypoxia, however, it inhibited the expression dose-dependently and significantly by up to 43% ($P < .05$; n = 3; Figure 3B).

VGSCα protein expression was studied using a pan-VGSC antibody since available "Nav1.7-specific" antibodies proved unsatisfactory. Immunocytochemistry and confocal image analyses were used to study effects of 2.5 µmol/L riluzole on plasma membrane expression under normoxia and hypoxia (Figure 4A). We focused on the plasma membrane since this is where the VGSC would be functional and contribute to invasiveness. In normoxia, riluzole had no effect on the plasma membrane expression. Under hypoxia, however, it increased VGSCα protein expression significantly by 16% ($P < .001$; n = 74 cells; Figure 4B).

## 4 | DISCUSSION

The main results of this study on rat PCa were as follows: (a) hypoxia had no effect on cell viability or proliferative activity at 24 hours; proliferation was reduced at 48 hours;

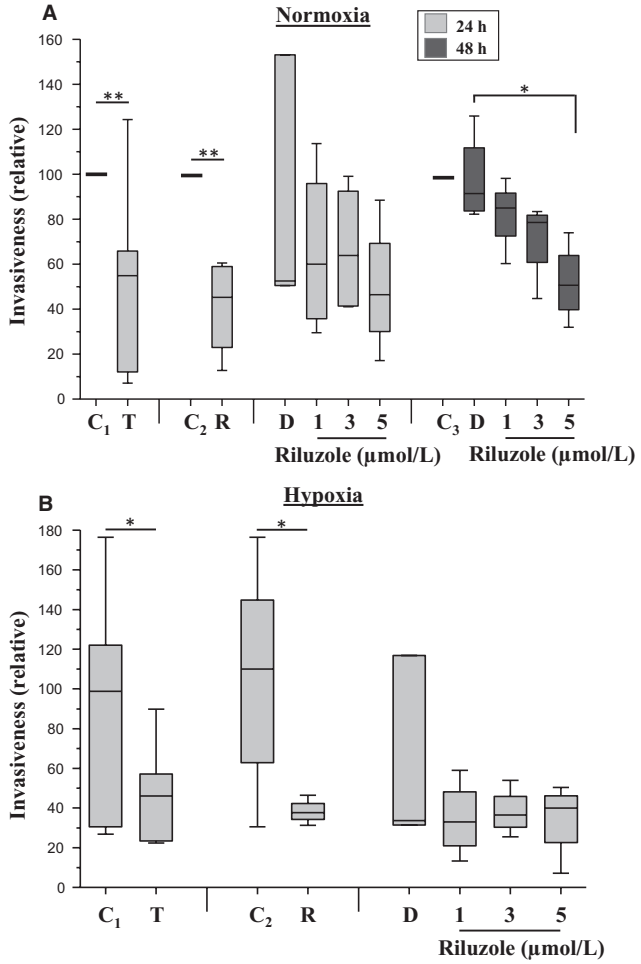


**FIGURE 2** Matrigel invasiveness of Mat-LyLu cells. Invasiveness was measured under normoxia (A) and hypoxic conditions (B) for 24 h (light bars) and 48 h (dark bars). Hypoxia was restricted to 24 h since cell growth was impaired at 48 h. $C_1$, media control for 1 µmol/L TTX (T). $C_2$, media control for 20 µM ranolazine (R). ($C_3$, media control for riluzole. D, DMSO control (0.0025%). Riluzole was applied at 1, 3 and 5 µmol/L. Data (normalized to the respective media control under normoxia) are presented as box plots (median values with 5 and 95% percentiles and interquartile ranges; n ≥ 3). Statistical significance: $P < .05$ (*); $P < .01$ (**)

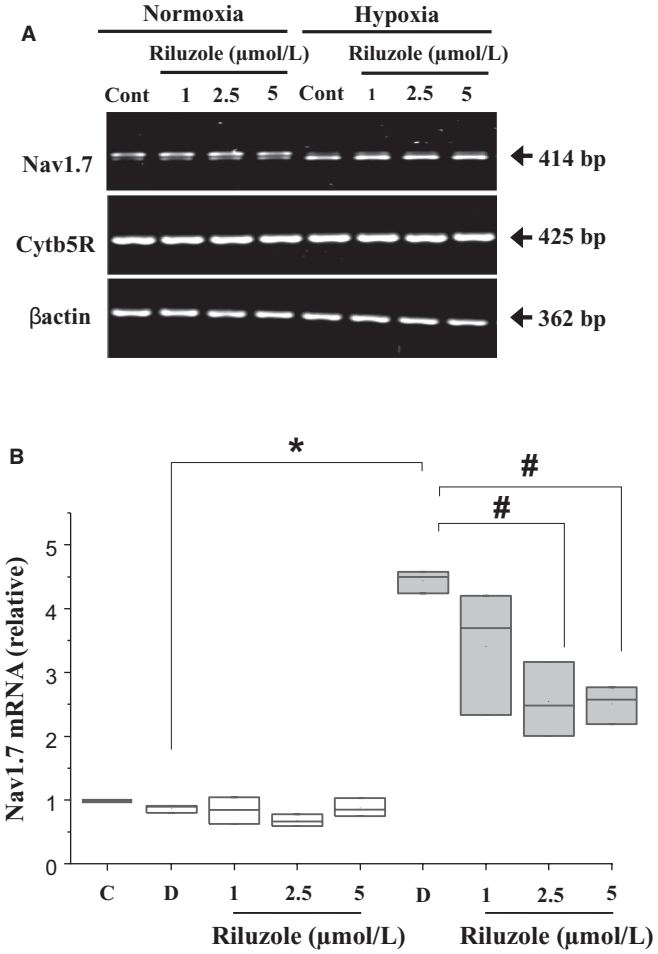


**FIGURE 3** Effects of riluzole on Nav1.7 mRNA expression in Mat-LyLu cells. A, Agarose gel electrophoresis of PCR products showing specific single bands of the expected sizes for Nav1.7 and the control genes, Cytb5R and β-actin (414, 425 and 362 nt, respectively). The "no-template control" did not give any signal (n = 3). B, Box diagrams show the result of real-time PCR experiment in which the effect of riluzole on Nav1.7 mRNA expression was studied under normoxic (white column) or hypoxic (light grey column) conditions. The data were normalized to Cytb5R using the $2^{-\Delta\Delta C_T}$ method and expressed relative to normoxic media control level. Analysis of variance (ANOVA) followed by Tukey's post hoc analysis and unpaired Student's *t* test were used for the statistical analysis. Data (normalized to the media control under normoxia) are presented as median values with 5 and 95% percentiles and interquartile ranges (n = 3). For pairwise significance: $P < .05$ for normoxia vs. hypoxia (*), and for control vs treatment (#). C, media control. D, DMSO control (0.0025%). Riluzole was applied at 1, 2.5 and 5 µmol/L

invasiveness was not affected (24 hours). (b) Riluzole (5 µmol/L), ranolazine (20 µmol/L) and TTX (1 µmol/L) had no effect on cell viability or proliferation (24 hours). (c) Matrigel invasion was inhibited by TTX and ranolazine (24 hours). (d) Riluzole also decreased invasion but significantly only after 48 hours of treatment; this effect could only be studied under normoxia since 48 hours in hypoxia by itself reduced cell number. (e) Nav1.7 mRNA expression was upregulated by hypoxia, whilst VGSCα protein level in plasma membrane was reduced. (f) Riluzole had no effect on Nav1.7 mRNA or VGSCα protein levels in normoxia; in hypoxia, Nav1.7 mRNA expression was significantly reduced (dose-dependently), whilst VGSCα protein in plasma membrane increased.

## 4.1 | Effects of hypoxia alone

The effects of 24 hours in hypoxia alone were consistent. No effect was seen on cellular morphology, viability or cell number. Interestingly, Nav1.7 mRNA expression was increased, whilst the plasma membrane VGSCα protein level decreased. This "mismatch" is discussed below. Surprisingly, hypoxia

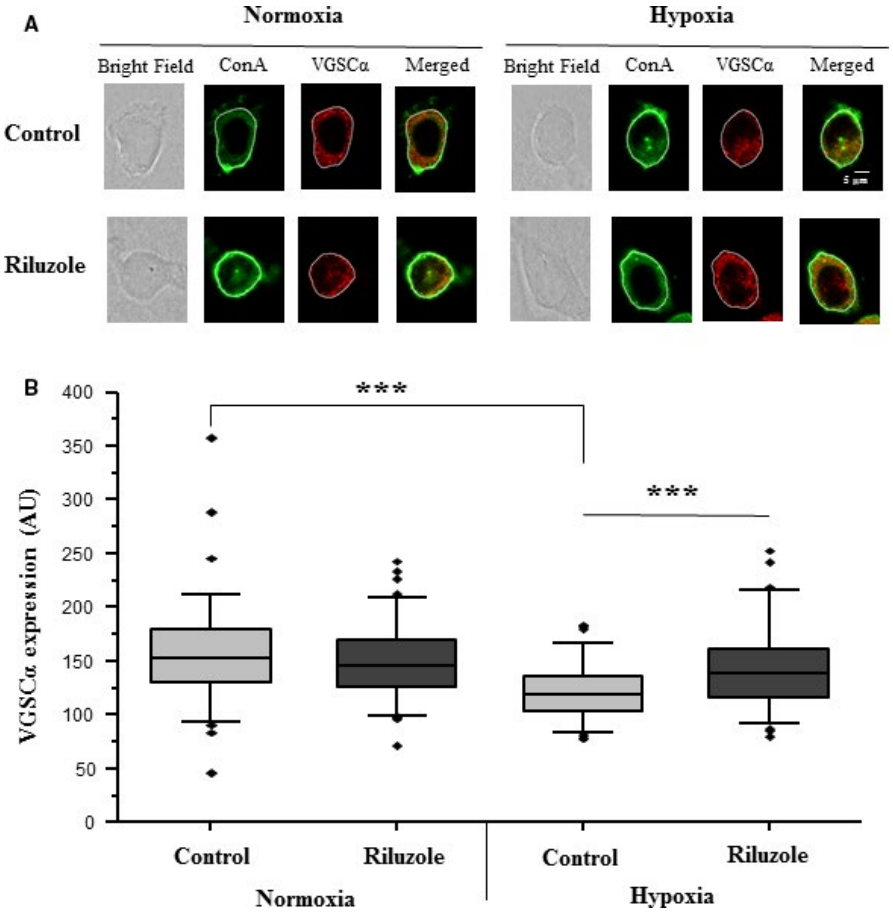


**FIGURE 4** Effects of riluzole on VGSCα protein expression in plasma membrane of Mat-LyLu cells. A, Typical XYZ confocal images of cells incubated for 24 h under normoxic and hypoxic (2% $O_2$) conditions with or without riluzole (2.5 μmol/L). Signal from concanavalin A (ConA) plasma membrane marker (green), pan-VGSCα antibody (red) and overlay of both (merged image) are shown in addition to bright-field images. Scale bar (5 μm) applicable to all panels. B, Data quantified from (A). Box plots showing VGSCα protein fluorescence levels (per μm) expressed in arbitrary unit (AU). Data are presented as median values with 5 and 95% percentiles, interquartile ranges and outliers. For each condition, 74-81 cells were measured from a minimum of three independent treatments. Statistical significance: $P < .001$ (***)

(24 hours) did not affect invasiveness although previous studies have shown hypoxia to promote the invasiveness of human PCa cells [eg[45,46]]. Indeed, the effect of hypoxia in promoting cellular invasiveness has been reported also for other cancers, for example colon,[34] breast[47,48] and gastric cancer.[49] The apparent lack of effect in the present study could be due to the "normoxic" Mat-LyLu cells also having some properties usually associated with hypoxia. These include HIF1α expression, reported earlier for human PCa (PC-3) cells, which share several characteristics with Mat-LyLu cells [eg[50-52]]. In addition, the current study was constrained by one major experimental limitation. The Boyden chamber technique had to be limited to 24 hours under hypoxia (in order to avoid the possible "contaminating" effect of the longer treatments inhibiting proliferation).

## 4.2 | Pharmacology

Riluzole, our main drug of interest, is an anti-excitatory and neuroprotective agent. It was proposed that the neuroprotective property of riluzole was via inhibition of the persistent component ($I_{NaP}$) of VGSC current.[53] Similarly, riluzole could protect against cardiac ischaemia by inhibiting $I_{NaP}$.[39] Riluzole binds to VGSC and stabilizes the channel in its inactivated state.[54,55] Consistent with the available data, riluzole was seen in the current study generally to be more effective in hypoxia. Ranolazine is also an inhibitor of $I_{NaP}$ and has been used clinically as an anti-angina drug.[32] Importantly, in this study we used concentrations of both riluzole and ranolazine that should fall within the therapeutic range. Thus, for riluzole, it has been estimated that it is not harmful to human beings at concentrations up to 10 μmol/L.[38,39] For ranolazine, the therapeutic plasma concentrations have been estimated to be in the range 2-8 μmol/L.[56]

## 4.3 | Effects of Riluzole on MAT-LyLu cell behaviours

### 4.3.1 | Proliferative activity

Riluzole had an anti-proliferative effect on Mat-LyLu cells, but this occurred at concentrations higher than that (5 μmol/L) required to inhibit invasiveness. Abdul and Hoosein initially studied four different PCa cell lines, including the VGSC-expressing human PC-3 cells and found that riluzole inhibited growth with an $IC_{50}$ of 43-128 μmol/L.[1] Akamatsu et al also showed that riluzole (10-50 μmol/L) induced inhibition of DNA synthesis and

apoptotic cell death via endoplasmic reticulum stress in both LNCaP and C4-2 cell lines.[57] It was also found that 25 μmol/L riluzole inhibited proliferation of melanoma cells and this occurred via inhibition of glutamate release, as suggested also for synapses.[39,58,59] In contrast, Parihar et al found that riluzole evoked concentration-dependent increases in proliferation of PC-3 and LNCaP cells with an $EC_{50}$ of 2 μmol/L.[60] This effect was proposed to be through intermediate-conductance $K_{Ca}$ channels, as shown for spinal neurones.[61] These data would suggest that concentrations of riluzole less than 10 μmol/L would not affect proliferation, whilst higher concentrations may be inhibitory through several mechanisms. The exception is the study of Parihar et al for which the reason(s) is not presently clear.[60] Nevertheless, in order to avoid any proliferative effect (and to keep to around the clinical dose), our Matrigel invasion assays were carried out with riluzole concentrations of only 1-5 μmol/L.

### 4.3.2 | Invasiveness

Here, we have shown that 5 μmol/L riluzole inhibited Matrigel invasion of Mat-LyLu cells, seen after 48 h in normoxia (possible effect in hypoxia over this time period could not be studied due to involvement of proliferation). Previous work on PC-3 and DU-145 cells showed similar anti-invasive effects of riluzole at concentrations greater than 10 μmol/L.[58] Riluzole (25 μmol/L) also suppressed melanoma invasiveness. These effects were suggested to occur through suppression of glutamate release which may be controlled by VGSC activity. More recent work on BCa cells showed, however, that the anti-invasive effect of riluzole could not be mediated by metabotropic glutamate receptors.[31,62] We should emphasize that in our experimental design, riluzole produced an anti-invasive effect without affecting proliferative activity. This is consistent with the notion that primary tumorigenesis and secondary tumorigenesis are controlled differently, perhaps even independently.[17,18,63]

### 4.3.3 | VGSC (Nav1.7) mRNA and protein expression

Riluzole significantly decreased Nav1.7 mRNA expression under only hypoxia. The VGSCα level in plasma membrane also was only affected under hypoxia but increased. In the first instance, again, this is consistent with the underlying mechanisms of action or riluzole being inhibition of VGSC/ $I_{NaP}$, well known to be promoted by hypoxia.[64,65] This would also agree overall with VGSC activity not being involved in PCa cell proliferation.[2,3,14] Regarding the mRNA and protein levels changing in different directions, it is now generally accepted that mRNA and protein expression can be regulated differentially and independently in cells, such that (a) mRNA can be produced and "docked" without being translated and (b) protein synthesis can occur later from such stored mRNA without necessitating prior transcription.[66-71] Previously, Brackenbury and Djamgoz also showed in Mat-LyLu cells that nerve growth factor up-regulated VGSC protein expression without any change in Nav1.7 mRNA expression.[72] Such differential regulation would depend on intracellular factors such as mRNA stability and protein lifetime [eg[73,74]]. The presumed mRNA "docking" process would be functionally expedient and particularly important pathophysiologically in cancer cells exposed to a wide variety of micro-environmental conditions. The relative levels of mRNA and protein may thus be optimized dynamically depending on time and space within the complexity of the cancer process. We should add, for completeness, that two other issues could have been involved in the "mRNA-protein" mismatch: (a) the protein level was measured only in the plasma membrane, whilst mRNA was total; and (b) any protein produced could have been subject to activity-dependent intracellular trafficking.[8]

## 5 | CONCLUSION

In overall conclusion, riluzole at clinical doses can inhibit PCa invasiveness in vitro without affecting cell viability or proliferative activity. These findings complement recent studies showing that another $I_{NaP}$ blocker, ranolazine, can suppress PCa and breast cancer metastasis in vivo,[16,33] and colon and breast cancer invasiveness in vitro.[34,75] These results may have wide-ranging impact for at least two reasons. Firstly, several other carcinomas are known to express functional VGSCs in vitro and in vivo, for example lung, cervix, stomach, melanoma and ovary [eg[19]]. Secondly, $I_{NaP}$ is likely to be a property of TTX-resistant and TTX-sensitive classes of VGSC [eg[76,77]]. Taken all together, therefore, increasing evidence would support the notion that VGSC/ $I_{NaP}$ blockers can be repurposed clinically as anti-metastatic drugs against several carcinomas.[8,12,19,78,79]

### ACKNOWLEDGEMENTS

We would like to acknowledge continued financial support from the Pro Cancer Research Fund (PCRF) in the form of a rolling grant (MBAD, SPF). This study was supported by the Istanbul University Research Fund (project number: 21348 (SU).

### CONFLICT OF INTEREST

MBAD has a patent pending for use of blockers of the persistent component of the voltage-gated sodium channel as

anti-cancer agents. The other authors (NR, SU, SPF, SA) declare no conflict of interest.

## ORCID

*Mustafa B. A. Djamgoz* https://orcid.org/0000-0003-1435-8540

## REFERENCES


1. Abdul M, Hoosein N. Voltage-gated sodium ion channels in prostate cancer: expression and activity. *Anticancer Res.* 2002;22:1727-1730.
2. Grimes JA, Fraser SP, Stephens GJ, et al. Differential expression of voltage-activated $Na^+$ currents in two prostatic tumour cell lines: contribution to invasiveness in vitro. *FEBS Lett.* 1995;369:290-294.
3. Laniado ME, Lalani EN, Fraser SP, et al. Expression and functional analysis of voltage-activated $Na^+$ channels in human prostate cancer cell lines and their contribution to invasion in vitro. *Am J Pathol.* 1997;150:1213-1221.
4. Nakajima T, Kubota N, Tsutsumi T, et al. Eicosapentaenoic acid inhibits voltage-gated sodium channels and invasiveness in prostate cancer cells. *Br J Pharmacol.* 2009;156:420-431.
5. Ding Y, Brackenbury WJ, Onganer PU, et al. Epidermal growth factor upregulates motility of Mat-LyLu rat prostate cancer cells partially via voltage-gated $Na^+$ channel activity. *J Cell Physiol.* 2008;215:77-81.
6. Diss JKJ, Stewart D, Pani F, et al. A potential novel marker for human prostate cancer progression: Voltage-gated $Na^+$ channel expression in vivo. *Prostate Cancer Prostatic Dis.* 2005;8:266-273.
7. Bennett ES, Smith BA, Harper JM. Voltage-gated $Na^+$ channels confer invasive properties on human prostate cancer cells. *Pflugers Arch Eur J Physiol.* 2004;44:908-914.
8. Brackenbury WJ, Djamgoz MBA. Activity-dependent regulation of voltage-gated $Na^+$ channel expression in Mat-LyLu rat prostate cancer cell line. *J Physiol.* 2006;573:343-356.
9. Djamgoz MBA, Mycielska M, Madeja Z, Fraser SP, Korohoda W. Directional movement of rat prostatic cancer cells in direct-current electric field: involvement of voltage-gated $Na^+$ channel activity. *J Cell Sci.* 2001;114:2697-2705.
10. Fraser SP, Salvador V, Manning E, et al. Contribution of functional voltage-gated $Na^+$ channel expression to cell behaviours involved in the metastatic cascade in rat prostate cancer: I. Lateral motility. *J Cell Physiol.* 2003;195:479-487.
11. Fraser SP, Diss JKJ, Chioni AM, et al. Voltage-gated sodium channel expression and potentiation of human breast cancer metastasis. *Clin Cancer Res.* 2005;11:5381-5389.
12. Gillet L, Roger S, Besson P, et al. Voltage-gated sodium channel activity promotes cysteine cathepsin-dependent invasiveness and colony growth of human cancer cells. *J Biol Chem.* 2009;284:8680-8691.
13. Mycielska ME, Fraser SP, Szatkowski M, Djamgoz MBA. Contribution of functional voltage-gated $Na^+$ channel expression to cell behaviours involved in the metastatic cascade in rat prostate cancer: II. Secretory membrane activity. *J Cell Physiol.* 2003;195:461-469.
14. Yildirim S, Altun S, Gumushan H, Patel A, Djamgoz MBA. Voltage-gated sodium channel activity promotes prostate cancer metastasis in vivo. *Cancer Lett.* 2012;323:58-61.
15. Bugan I, Karagoz Z, Altun S, Djamgoz MBA. Gabapentin, an analgesic used against cancer-associated neuropathic pain: effects on prostate cancer progression in an in vivo rat model. *Basic Clin Pharmacol Toxicol.* 2016;118:200-207.
16. Bugan I, Kucuk S, Karagoz Z, et al. Anti-metastatic effect of ranolazine, in an *in vivo* rat model of prostate cancer, and expression of voltage-gated sodium channel protein in human prostate. *Prostate Cancer Prostatic Dis.* 2019;22:569-579.
17. Welch DR. Microarrays bring new insights into understanding of breast cancer metastasis to bone. *Breast Cancer Res.* 2004;6:61-64.
18. Welch DR. Do we need to redefine a cancer metastasis and staging definitions? *Breast Dis.* 2006;26:3-12.
19. Djamgoz MBA, Fraser SP, Brackenbury WJ. In vivo evidence for expression of voltage-gated sodium channels in cancer and potentiation of metastasis. *Cancers* 2019;11:E1675.
20. Koltai T. Voltage-gated sodium channel as a target for metastatic risk reduction with re-purposed drugs. *F1000Res.* 2015;4:297.
21. Martin F, Ufodiama C, Watt I, Bland M, Brackenbury WJ. Therapeutic value of voltage-gated sodium channel inhibitors in breast, colorectal, and prostate cancer: a systematic review. *Front Pharmacol.* 2015;6:273.
22. Djamgoz MBA, Onkal R. Persistent current blockers of voltage-gated sodium channels: a clinical opportunity for controlling metastatic disease. *Recent Pat Anticancer Drug Discov.* 2013;8:66-84.
23. de Lera RM, Kraus RL. Voltage-gated sodium channels: Structure, function, pharmacology and clinical indications. *J Med Chem.* 2015;58:7093-7118.
24. Fraser SP, Foo I, Djamgoz MBA. Local anaesthetic use in cancer surgery and disease recurrence: role of voltage-gated sodium channels? *Br J Anaesth.* 2014;113:899-902.
25. Yang M, Kozminski DJ, Wold LA, et al. Therapeutic potential for phenytoin: Targeting Na(v)1.5 sodium channels to reduce migration and invasion in metastatic breast cancer. *Breast Cancer Res Treat.* 2012;134:603-615.
26. Nagoshi N, Nakashima H, Fehlings MG. Riluzole as a neuroprotective drug for spinal cord injury: From bench to bedside. *Molecules* 2015;20:7775-7789.
27. Bensimon G, Lacomblez L, Meininger, . V. A controlled trial of riluzole in amyotrophic lateral sclerosis. *N Engl J Med.* 1994;330:585-591.
28. Taguchi YH, Wang H. Genetic association between amyotrophic lateral sclerosis and cancer. *Genes (Basel).* 2017;8:E243.
29. Lemieszek MK, Stepulak A, Sawa-Wejksza K, Czerwonka A, Ikonomidou C, Rzeski W. Riluzole inhibits proliferation, migration and cell cycle progression and induces apoptosis in tumor cells of various origins. *Anticancer Agents Med Chem.* 2018;18:565-572.
30. Le MN, Chan J-K, Rosenberg SA, et al. The glutamate release inhibitor Riluzole decreases migration, invasion, and proliferation of melanoma cells. *J Invest Dermatol.* 2010;130:2240-2249.
31. Speyer CL, Nassar MA, Hachem AH, et al. Riluzole mediates anti-tumor properties in breast cancer cells independent of metabotropic glutamate receptor-1. *Breast Cancer Res Treat.* 2016;157:217-228.
32. Belardinelli L, Shryock JC, Fraser H. Inhibition of the late sodium current as a potential cardioprotective principle: effects of the late sodium current inhibitor ranolazine. *Heart.* 2006;92(suppl_4):iv6-iv14.

33. Driffort V, Gillet L, Bon E, et al. Ranolazine inhibits Nav1.5-mediated breast cancer cell invasiveness and lung colonization. *Mol Cancer.* 2014;13:264-269.
34. Guzel RM, Ogmen K, Ilieva KM, Fraser SP, Djamgoz MBA. Colorectal cancer invasiveness in vitro: Predominant contribution of neonatal Nav1.5 under normoxia and hypoxia. *J Cell Physiol.* 2019;234:6582-6593.
35. Rankin EB, Giaccia AJ. Hypoxic control of metastasis. *Science.* 2016;352:175-180.
36. Karagiannis GS, Pastoriza JM, Wang Y, et al. Neoadjuvant chemotherapy induces breast cancer metastasis through a TMEM-mediated mechanism. *Sci Transl Med.* 2017;9:397.
37. Karagiannis GS, Condeelis JS, Oktay MH. Chemotherapy-induced metastasis: mechanisms and translational opportunities. *Clin Exp Metastasis.* 2018;35:269-284.
38. Le Liboux A, Cachia JP, Kirkesseli S, et al. A comparison of the pharmacokinetics and tolerability of riluzole after repeat dose administration in healthy elderly and young volunteers. *J Clin Pharmacol.* 1999;39:480-486.
39. Weiss S, Benoist D, White E, Teng W, Saint DA. Riluzole protects against cardiac ischaemia and reperfusion damage via block of the persistent sodium current. *Br J Pharmacol.* 2010;160:1072-1082.
40. Mycielska ME, Palmer CP, Brackenbury WJ, Djamgoz MBA. Expression of $Na^+$-dependent citrate transport in a strongly metastatic human prostate cancer PC-3M cell line: regulation by voltage-gated $Na^+$ channel activity. *J Physiol.* 2005;563:393-408.
41. Seda M, Pinto FM, Wray S, et al. Functional and molecular characterization of voltage-gated sodium channels in uteri from nonpregnant rats. *Biol Reprod.* 2007;77:855-863.
42. Brackenbury WJ, Chioni AM, Diss JKJ, Djamgoz MBA. The neonatal splice variant of Nav1.5 potentiates in vitro invasive behaviour of MDA-MB-231 human breast cancer cells. *Breast Cancer Res Treat.* 2007;101:149-160.
43. Krawetz S. *Bioinformatics for Systems Biology*. New York, NY: Humana Press, 2009.
44. Livak KJ, Schmittgen TD. Analysis of relative gene expression data using real-time quantitative PCR and the 2(-Delta Delta C(T)) method. *Methods.* 2001;25:402-408.
45. Iwasaki K, Ninomiya R, Shin T, et al. Chronic hypoxia-induced slug promotes invasive behavior of prostate cancer cells by activating expression of ephrin-B1. *Cancer Sci.* 2018;109:3159-3170.
46. Lee JE, Shin SH, Shin HW, Chun YS, Park JW. Nuclear FGFR2 negatively regulates hypoxia-induced cell invasion in prostate cancer by interacting with HIF-1 and HIF-2. *Sci Rep.* 2019;9:3480.
47. Hoffmann C, Mao X, Brown-Clay J, et al. Hypoxia promotes breast cancer cell invasion through HIF-1α-mediated up-regulation of the invadopodial actin bundling protein CSRP2. *Sci Rep.* 2018;8:10191.
48. Muñoz-Nájar UM, Neurath KM, Vumbaca F, Claffey KP. Hypoxia stimulates breast carcinoma cell invasion through MT1-MMP and MMP-2 activation. *Oncogene.* 2006;25:2379-2392.
49. Liu HL, Liu D, Ding GR, Liao PF, Zhang JW. Hypoxia-inducible factor-1α and Wnt/β-catenin signaling pathways promote the invasion of hypoxic gastric cancer cells. *Mol Med Rep.* 2015;12:3365-3373.
50. Ranasinghe WKB, Baldwin GS, Bolton D, Shulkes A, Ischia J, Patel O. HIF1α expression under normoxia in prostate cancer - Which pathways to target? *J Urol.* 2015;193:763-770.
51. Saramäki OR, Savinainen KJ, Nupponen NN, Bratt O, Visakorpi T. Amplification of hypoxia-inducible factor 1 alpha gene in prostate cancer. *Cancer Genet Cytogenet.* 2001;128:31-34.
52. Siegsmund MJ, Kreukler C, Steidler A, Nebe T, Köhrmann KU, Alken P. Multidrug resistance in androgen-independent growing rat prostate carcinoma cells is mediated by P-glycoprotein. *Urol Res.* 1997;25:35-41.
53. Urbani A, Belluzi O. Riluzole inhibits the persistent sodium current in mammalian CNS neurons. *Eur J Neurosci.* 2000;12:3567-3574.
54. Doble A. The role of excitotoxicity in neurodegenerative disease: implications for therapy. *Pharmacol Ther.* 1999;81:163-221.
55. Hebert T, Drapeau P, Pradier L, Dunn RJ. Block of the rat brain IIA sodium channel alpha subunit by the neuroprotective drug riluzole. *Mol Pharmacol*. 1994;45:1055-1060.
56. Rajamani S, Shryock JC, Belardinelli L. Block of tetrodotoxin-sensitive, Nav1.7 and tetrodotoxin-resistant, Nav1.8, $Na^+$ channels by ranolazine. *Channels (Austin).* 2008;2:449-460.
57. Akamatsu K, Shibata MA, Ito Y, Sohma Y, Azuma H, Otsuki Y. Riluzole induces apoptotic cell death in human prostate cancer cells via endoplasmic reticulum stress. *Anticancer Res.* 2009;29:2195-2204.
58. Koochekpour S, Majumdar S, Azabdaftari G, et al. Serum glutamate levels correlate with Gleason score and glutamate blockade decreases proliferation, migration, and invasion and induces apoptosis in prostate cancer cells. *Clin Cancer Res.* 2012;18:5888-5901.
59. Lamanauskas N, Nistri A. Riluzole blocks persistent $Na^+$ and $Ca^{2+}$ currents and modulates release of glutamate via presynaptic NMDA receptors on neonatal rat hypoglossal motoneurons in vitro. *Eur J Neurosci.* 2008;27:2501-2514.
60. Parihar AS, Coghlan MJ, Gopalakrishnan M, Shieh CC. Effects of intermediate-conductance $Ca^{2+}$-activated $K^+$ channel modulators on human prostate cancer cell proliferation. *Eur J Pharmacol.* 2003;471:157-164.
61. Dimitriadi M, Kye MJ, Kalloo G, Yersak JM, Sahin M, Hart AC. The neuroprotective drug riluzole acts via small conductance $Ca^{2+}$-activated $K^+$ channels to ameliorate defects in spinal muscular atrophy models. *J Neurosci.* 2013;33:6557-6562.
62. Dolfi SC, Medina DJ, Kareddula A, et al. Riluzole exerts distinct antitumor effects from a metabotropic glutamate receptor 1-specific inhibitor on breast cancer cells. *Oncotarget.* 2017;8:44639-44653.
63. Welch DR, Steeg PS, Rinker-Schaeffer CW. Rinker-Schaeffer CW. Molecular biology of breast cancer metastasis. Genetic regulation of human breast carcinoma metastasis. *Breast Cancer Res.* 2000;2:408-416.
64. Fearon IM, Brown ST. Acute and chronic hypoxic regulation of recombinant hNa(v)1.5 alpha subunits. *Biochem Biophys Res Commun.* 2004;324:1289-1295.
65. Hammarström AK, Gage PW. Hypoxia and persistent sodium current. *Eur Biophys J.* 2002;31:323-330.
66. Gu X, Lundqvist EN, Coates PJ, Thurfjell N, Wettersand E, Nylander K. Dysregulation of TAp63 mRNA and protein levels in psoriasis. *J Invest Dermatol.* 2006;126:137-141.
67. Martin KC, Zukin RS. RNA trafficking and local protein synthesis in dendrites: An overview. *J Neurosci.* 2006;26:7131-7134.
68. Orphanides G, Reinberg D. A unified theory of gene expression. *Cell.* 2002;108:439-451.
69. Pfeiffer BE, Huber KM. Current advances in local protein synthesis and synaptic plasticity. *J Neurosci.* 2006;26:7147-7150.

70. Schedel J, Distler O, Woenckhaus M, et al. Discrepancy between mRNA and protein expression of tumour suppressor maspin in synovial tissue may contribute to synovial hyperplasia in rheumatoid arthritis. *Ann Rheum Dis.* 2004;63:1205-1211.
71. Sola B, Salün V, Ballet JJ, Troussard X. Transcriptional and post-transcriptional mechanisms induce cyclin-D1 over-expression in B-chronic lymphoproliferative disorders. *Int J Cancer.* 1999;83:230-234.
72. Brackenbury WJ, Djamgoz MBA. Nerve growth factor enhances voltage-gated $Na^+$ channel activity and transwell migration in Mat-LyLu rat prostate cancer cell line. *J Cell Physiol.* 2007;210:602-608.
73. Ben Fredj N, Grange J, Sadoul R, Richard S, Goldberg Y, Boyer V. Depolarization-induced translocation of the RNA-binding protein Sam68 to the dendrites of hippocampal neurons. *J Cell Sci.* 2004;117:1079-1090.
74. St JD. Moving messages: The intracellular localization of mRNAs. *Nat Rev Mol Cell Biol.* 2005;6:363-375.
75. Lee A, Fraser SP, Djamgoz MBA. Propranolol inhibits neonatal Nav1.5 activity and invasiveness of MDA-MB-231 breast cancer cells: Effects of combination with ranolazine. *J Cell Physiol.* 2019;234:23066-23081.
76. Yamanishi T, Koizumi H, Navarro MA, Milescu LS, Smith JC. Kinetic properties of persistent $Na^+$ current orchestrate oscillatory bursting in respiratory neurons. *J Gen Physiol.* 2018;150:1523-1540.
77. Yao L, Fan P, Jiang Z, et al. Nav1.5-dependent persistent $Na^+$ influx activates CaMKII in rat ventricular myocytes and N1325S mice. *Am J Physiol Cell Physiol.* 2011;301:C577-586.
78. Onkal R, Djamgoz MBA. Molecular pharmacology of voltage-gated sodium channel expression in metastatic disease: Clinical potential of neonatal Nav1.5 in breast cancer. *Eur J Pharmacol.* 2009;625:206-219.
79. Roger S, Potier M, Vandier C, Besson P, Le Guennec JY. Voltage-gated sodium channels: New targets in cancer therapy? *Curr Pharm Des.* 2006;12:3681-3695.

**How to cite this article:** Rizaner N, Uzun S, Fraser SP, Djamgoz MBA, Altun S. Riluzole: Anti-invasive effects on rat prostate cancer cells under normoxic and hypoxic conditions. *Basic Clin Pharmacol Toxicol*. 2020;127:254–264. https://doi.org/10.1111/bcpt.13417